# Numerical Study of Polymer Force-Extension Relationship in a High-Frequency Electric Field

William E. Uspal[1]
[1] *Massachusetts Institute of Technology, Cambridge, Massachusetts 02139, USA*
(Dated: May 15, 2009)

Through a numerical bead-rod model, we examine the force-extension relationship for a polymer in a high frequency AC field. We find preliminary agreement with the theoretical model of Cohen, in which the addition of a nematic potential to the worm-like chain Hamiltonian produces sine-Gordon solitons, representing kinks and antikinks in the polymer contour. We observe and comment on features in the conformation and dynamics of the polymer.

PACS numbers:

The last decade has seen explosive growth in force spectroscopy of single biomacromolecules, allowing researchers to probe the free energy landscape and dynamics of RNA, proteins, and DNA, without having important phenomena obscured by the ensemble averaging inherent in bulk techniques.[1, 2] This growth has most obviously been driven by the invention and subsequent refinement of experimental techniques like atomic force microscopy (AFM) and optical trapping, but developments in both theoretical nonequilibrium statistical physics and computational modeling have provided a significant spur to experimental work. For instance, the recently formulated Jarzynski equality has been of great value in the study of RNA denaturation.

It is in light of this interplay between theory, numerical modeling, and experiment that we approach the study of polymers in high frequency AC electric fields. Using high frequency fields is of increasing interest in the experimental manipulation of biological material.[3] Spatially inhomogeneous fields, whether AC or DC, can act on neutral particles in a phenomenon called dielectrophresis (DEP); the imposed field $\boldsymbol{E}$ induces a polarization $\boldsymbol{p}$, upon which the field can act:

$$\boldsymbol{F} = (\boldsymbol{p} \cdot \bigtriangledown)\boldsymbol{E}. \tag{1}$$

The effect is therefore second order in $\boldsymbol{E}$. AC fields are of particular value for several reasons. They do not carry the adverse ionic screening effects of DC fields. Secondly, whether their effect is attractive or repulsive depends on frequency $\omega$ and a characteristic $\omega_c$ of the material, an effect which has been exploited in the separation of biological material.

However, experimenters have noted anomalous behavior in polyelectrolytes which cannot be accounted for in the theory of dielectrophresis of a particle without internal structure. In particular, DNA tethered to an electrode was found to extend to its full contour length, though naively the potential should have been attractive. In this connection, Cohen examined, on the basis of statistical mechanics, the conformation of a polymer in a high frequency AC field.[4]

Cohen's theory, described more extensively in the next section, revealed that the bending potential of the worm-like chain (WLC) is crucial to AC field-driven spontaneous extension to the full polymer contour length. The effect of the field on a freely jointed chain (FJC) is only to alter the aspect ratio of the polymer coil, with the strong field limit being a random walk in one dimension. Furthermore, contours that minimize the energy of a WLC in a field are soliton hairpin kinks, in which the polymer reverses alignment with the field over a characteristic length scale $s_0$, and with a characteristic energy $U_k$. Having well defined length and energy, kinks can be considered particles, and Cohen derives a polymer force-extension relationship on the basis of kink gas statistics.

In this letter, we provide evidence for aspects of Cohen's theory via numerical simulation of bead-rod chains. Furthermore, we observe structural and dynamic phenomena which may provide direction for continued numerical research. These phenomena are most likely not amenable to full analytical treatment, so that further numerical study may, in turn, be positioned to provide direction for experimental work.

## Theory

As Cohen argues, for long chains we may assume linear polarizability $\alpha$. The local polarization density in a spatially homogeneous field $\boldsymbol{E} = E\hat{x}$ is $d\boldsymbol{p}(s) = \alpha(\boldsymbol{E} \cdot \boldsymbol{u})d\boldsymbol{u}$, where $\boldsymbol{u}(s)$ is the unit vector tangent to the chain at point $s$ along the contour. The time averaged electrostatic free energy density is

$$U_n(s) = -V\cos^2(\theta(s)) \tag{2}$$

with $V = \frac{1}{2}\alpha E^2$ and $\theta(s) = (\boldsymbol{u} \cdot \hat{x})$.

Immediately, one may note that there are two potential minima for this term: alignment and anti-alignment with the field direction. The associated force is in the direction of the closer orientation. A similar $\cos^2(\theta(s))$ term arises in the theory of nematic polymer liquid crystals; hence the designation $U_n$.

Cohen first examines the weak tension and weak field regime, in which it is acceptable to model DNA as a FJC. Cohen writes the single rod partition function, which may be exactly evaluated in terms of error functions. In the weak field limit, the dumbbell spring constant in the field direction is softened to

$$k \approx \frac{3k_BT}{Lb} - \frac{4V}{5L} \tag{3}$$

leading to a biased random walk, and accordingly a larger radius of gyration in the $\hat{x}$ direction:

$$R_G^2 = \frac{Nb^2}{3} + \frac{4NVb^3}{45k_BT}. \tag{4}$$

One can easily see that, in the strong field limit, the polymer collapses to a one dimensional random walk, and is not fully extended.

The FJC fails to capture the spontaneous extension of DNA because it neglects bending rigidity, which provides strong energetic penalty for reversal of alignment of neighboring rods. Thus it is necessary to move to the (continuum) WLC description of chain energy:

$$H = \int_0^L \left( \frac{1}{2}\kappa \left| \frac{\partial \boldsymbol{u}}{\partial s} \right|^2 - V\cos^2(\theta) \right) ds \tag{5}$$

As shown by de Gennes, the sine-Gordon soliton minimizes this Hamiltonian:

$$\theta_{hp}(s) = 2\cot^{-1}(exp(-s/s_0)) \tag{6}$$

where $s_0$, the characteristic size, is $\sqrt{\kappa/2V} = \sqrt{l_p k_B T/2V}$. These are hairpin kinks and antikinks in the WLC contour, in which the chain switches alignment with the field over a length scale $s_0$. Kinks and antikinks must alternate. The characteristic energy can be obtained by substituting Equation 6 in Equation 5:

$$U_k = 2\sqrt{2\kappa V} = 2k_BT\frac{l_p}{s_0}. \tag{7}$$

Cohen obtains the force-extension relationship by considering the statistics of a kink gas. Without imposed force, an equilibrium number of kinks is thermally activated:

$$n_{eq}^0 = 16(LV/k_BT)exp(-U_k/k_BT) \tag{8}$$

where the prefactor takes into account a reorientation attempt length $l^* = k_BT/16V$, found elsewhere by an analogy with quantum mechanical tunneling in a rigid rotor.

Cohen maps the problem onto a 1D Ising spin chain to find an estimate for the force-extension curve. Kinks constitute domain walls, while an imposed force corresponds to a magnetic field. This yields a force-extension curve

$$x_0/L = \left[ 1 + \left( \frac{k_BTn_{eq}^0}{FL} \right)^2 \right]^{-1/2}. \tag{9}$$

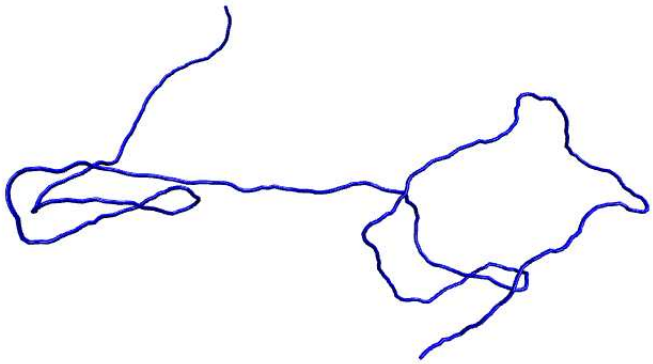

FIG. 1: A snapshot of kinked DNA, obtained for a simulation with $N_b = 400$, $l_p = 15$, giving $L = 1.41\mu m$, and $Vl_p = 3.75$.

The polymer is extended to nearly full contour length rather easily. Cohen also derives an expression taking into account thermal fluctuations between kinks, which leads to a reduction in extension for a given force:

$$x = x^+ - x^- \tag{10}$$

where

$$x^{\pm} = L^{\pm}\left(1 - \sqrt{\frac{k_BT}{4l_pF_{eff}^{\pm}}}\right), \tag{11}$$

$$L^{\pm} = (L \pm x_0)/2. \tag{12}$$

and

$$F_{eff}^{\pm} = 2V \pm F. \tag{13}$$

We are now in a position to explain the experimentally observed spontaneous extension. A sufficiently strong field may send $n_{eq}^0$ in Equation 8 to $n_{eq}^0 \ll 1$, since the term is exponentially surpressed by $U_k = 2\sqrt{2\kappa V}$.

## Numerical Method

We study polymer force-extension behavior via Brownian Dynamics (BD) simulations of bead-rod chains. Internal and external forces on the chain act are applied to the beads, which are connected by massless inextensible rods. In this study, external forces include the drag of the solvent and dielectrophoretic force of the AC field. We assume chains are free draining, omitting long-range hydrodynamic interactions. Internal forces include chain bending rigidity and the set of tensions needed to maintain fixed rod length. Bending rigidity is omitted in the freely jointed chain (FJC) and included in the discretized worm-like chain (WLC).

In BD, chain time evolution is determined by a set of $N_b$ Langevin equations:

$$d\boldsymbol{r}_i = \left[\frac{1}{\zeta}(\boldsymbol{F}^i_{DE} + \boldsymbol{F}^i_C + \boldsymbol{F}^i_B)\right] dt + \sqrt{\frac{2kT}{\zeta}} d\boldsymbol{W}_i \quad (14)$$

for $i = 1, .., N_b$ beads. $F^i_{DE}$, $F^i_B$, and $F^i_C$ are the dielectrophoretic, bending, and constraint forces, respectively, which are scaled by the drag coefficient $\zeta$. The second term, $d\boldsymbol{W}_i$, provides thermal noise, with correlations $\langle d\boldsymbol{W}_i(t)\rangle = 0$ and $\langle d\boldsymbol{W}_i(t) d\boldsymbol{W}_j(t')\rangle = dt\delta_{ij}\delta(t-t')\boldsymbol{\delta}$ for beads $j = 1, .., N_b$.

The set of forces $\boldsymbol{F}^i_C$ are not known *a priori*, but are such as to impose the set of $N_b - 1$ constraints

$$(\boldsymbol{r}_{i+1} - \boldsymbol{r}_i) \cdot (\boldsymbol{r}_i - \boldsymbol{r}_{i-1}) - b^2 = 0 \quad (15)$$

within a specified tolerance, where $b$ is the bond length. The need to simultaneously solve $2N_b - 1$ coupled equations makes stepping forward in time a non-trivial problem. We adopt the predictor-corrector method of Somasi et al., [5] whereby we first make a predictor move with all other forces, and then iteratively solve for the forces of constraint.

First, however, we note that $b$ and $\zeta b^2/(k_B T)$ provide natural length and time scales for nondimensionalization of Equation 14, while energy and force should be considered in unis of $k_B T$ and $k_B T/b$. For convenience, equations in what follows are made dimensionless by these units.

The predictor move is a simple unconstrained Euler step:

$$\boldsymbol{r}^*_i = \boldsymbol{r}_i(t) + (\boldsymbol{F}^i_B + \boldsymbol{F}^i_{DE})\delta t + \sqrt{2}\boldsymbol{W} \quad (16)$$

We would like to obtain the next set of positions as

$$\boldsymbol{r}_i(t + \delta t) = \boldsymbol{r}^*_i + \boldsymbol{F}^i_C \delta t. \quad (17)$$

Furthermore, the forces $\boldsymbol{F}^i_C$ are supplied by a set of rod tensions $\{T_i\}$:

$$\boldsymbol{F}^i_C = T_i \boldsymbol{u}_i - T_{i-1}\boldsymbol{u}_{i-1} \quad (18)$$

where $\boldsymbol{u}_i$ is a unit bond vector $\boldsymbol{u}_i = (\boldsymbol{r}_{i+1} - \boldsymbol{r}_i)$. Combining equations 16, 17, and 18 and rearranging, we obtain a set of $N_b - 1$ nonlinear equations

$$\begin{aligned} A_i &= (2\delta t)\boldsymbol{q}_i \cdot (T_{i-1}\boldsymbol{u}_{i-1} - 2T_i\boldsymbol{u}_i + T_{i+1}\boldsymbol{u}_{i+1}) - 1 \\ &+ (\delta t)^2 (T_{i-1}\boldsymbol{u}_{i-1} + 2T_i\boldsymbol{u}_i + T_{i+1}\boldsymbol{u}_{i+1})^2 + (|\boldsymbol{q}_i|)^2 = 0 \end{aligned} \quad (19)$$

where $A_i$ is the $i$th equation, and $\boldsymbol{q}_i$ is a rod vector from the predictor step: $\boldsymbol{q}_i = (\boldsymbol{r}^*_{i+1} - \boldsymbol{r}^*_i)$. We define a vector of tension variables $\boldsymbol{T} = \{T_1, T_2, .., T_{N_b-1}\}$, and a vector of equations $\boldsymbol{A} = \{A_1, A_2, .., A_{N_b-1}\}$. Using Newton's method, we iteratively solve for $\boldsymbol{T}$ by

$$\boldsymbol{J}(\boldsymbol{T}^{old})(\boldsymbol{T}^{new} - \boldsymbol{T}^{old}) = -\boldsymbol{A}(\boldsymbol{T}^{old}) \quad (20)$$

where the Jacobian matrix is

$$\boldsymbol{J} = \frac{\partial \boldsymbol{A}}{\partial \boldsymbol{T}}. \quad (21)$$

Equation 20 gives a tridiagonal system, which can be solved with the Thomas algorithm. The method is iterated until $|\boldsymbol{T}^{new} - \boldsymbol{T}^{old}|$ is less than tolerance. We take the tolerance to be $10^{-7}$. This method requires an initial set of guesses for $\boldsymbol{T}$; we use the set from the previous simulation time step.

We have yet to specify the forces $\boldsymbol{F}^i_B$ and $\boldsymbol{F}^i_{DE}$. The first, applicable for the WLC, comes from the following (dimensional) term in the Hamiltonian:

$$H_{bending} = \int_0^L \frac{1}{2}\kappa \left|\frac{\partial \boldsymbol{u}}{\partial s}\right|^2 ds \quad (22)$$

where the bending modulus $\kappa = l_p k_B T$, and $l_p$ is the persistence length. Discretising this term, we find

$$H_{bending} = \frac{k_B T l_p}{2b} \sum_{k=1}^{N_b-2} (\boldsymbol{u}_{k+1} - \boldsymbol{u}_k)^2. \quad (23)$$

With

$$F^i_B = -\frac{\partial H_{bending}}{\partial \boldsymbol{r_i}} \quad (24)$$

we find that, now dimensionless,

$$F^i_B = l_p((\boldsymbol{u}_{i+1} - \boldsymbol{u}_i) - 2(\boldsymbol{u}_i - \boldsymbol{u}_{i-1}) + (\boldsymbol{u}_{i-1} - \boldsymbol{u}_{i-2})) \quad (25)$$

for $2 < i < (N_b - 2)$, and appropriate modifications for the end beads.

The dielectrophoretic term in the Hamiltonian is

$$H_{DEP} = -V \int_0^L (\boldsymbol{u}(s) \cdot \hat{x})^2 ds \quad (26)$$

which, discretized, gives

$$H_{DEP} = -Vb \sum_{k=1}^{N_b-1} (\boldsymbol{u}_k \cdot \hat{x})^2 \quad (27)$$

Taking a derivative as before, we find the (dimensionless) force

$$\boldsymbol{F}^i_{DE} = 2V\hat{x} \cdot (\boldsymbol{u}_{i-1} - \boldsymbol{u}_i)\hat{x} \quad (28)$$

for $1 < i < N_b$.

Parameters characterizing terms in the Hamiltonian, here dimensionless, are $V$ and $l_p$. Since the persistence length of DNA is $0.053\mu m$, $l_p$ actually sets the level of discretisation, and, together with $N_b$, the contour length studied. To reproduce the FJC curve, we take $N_b = 100$, and to reproduce the WLC curve, we further take $l_p = 5$, giving a chain with 10 Kuhn steps (a WLC Kuhn step is twice a persistence length.) Computational constraints

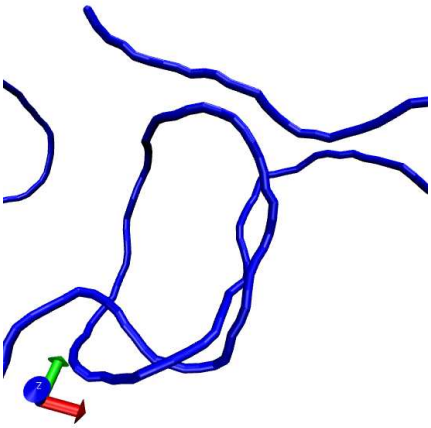

FIG. 2: Knot observed in the simulation of a chain with $N_b = 400$ and $l_p/b = 15$, for an approximate contour length of $L = 1.41\mu m$, and $Vl_p/k_BT = 3.75$. Whether knots form when bonds are non-phantom is a possible direction of further study.

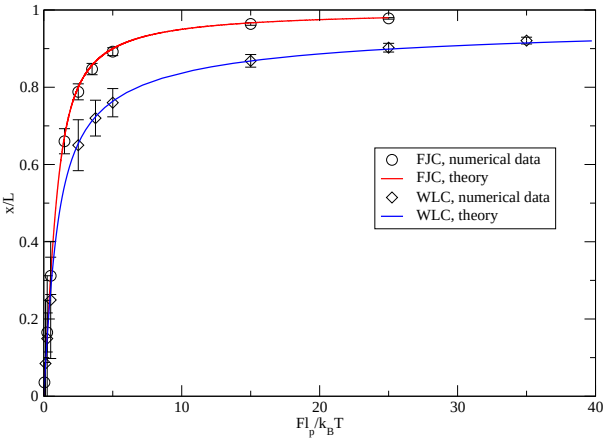


FIG. 3: We find good agreement between the force-extension data provided by our numerical model and theory for both the FJC and WLC.

did not allow for simulation of longer chains in the time available. For chains with the nematic potential, we fine grain further, setting $N_b = 200$ and $l_p = 10$, also yielding 10 Kuhn steps. We do so because adequating capturing the soliton length scale requires $1 \ll \sqrt{l_p/2V}$. For the force-extension curve with the nematic potential, we set $Vl_p = 6.0$ and vary $F_{ext}$. In studying the free kink gas, we set $F_{ext} = 0$ and vary $V$.

The dimensionless simulation timestep $\delta t$ we tune with level of discretisation; for instance, for $N_b = 200$ and $l_p = 10$, we set it as $\delta t = 5.0 \times 10^{-4}$.

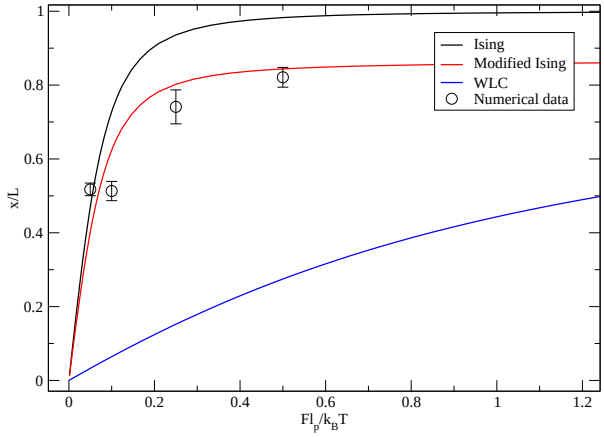


FIG. 4: Force-extension data with the nematic potential is still limited. Nevertheless, initial signs suggest agreement with the modified Ising curve.

### Results and Discussion

At the outset, we verified that our bead-rod model is sound by reproducing the well-known theoretical curves for the freely jointed and worm-like chains, shown in Figure 3. We find close agreement between the numerical results and the theoretical curves, including good collapse in the low extension, entropic spring region. The WLC curve is given by the Marko-Siggia formula

$$Fl_p/k_BT = \left[\frac{1}{4}(1 - x/L)^{-2} - \frac{1}{4} + x/L\right], \qquad (29)$$

which is an interpolation between low and high extension limits.[6]

Upon adding the nematic potential, we observed highly kinked conformations, such as in Figure 1. We planned to show localization of energy in kinks and motion thereof by plotting bending energy versus contour length as a function of time in a color map, but the data is too noisy, limiting our study of solitons in the kink gas regime to qualitative observation. Quantitative study of kinks, such as the number in equilibrium, or the dynamics of their diffusion and annihiliation, will require more extensive computation time as we further fine grain and examine longer contour lengths, so as to be closer to the long chain limit. An interesting structure we noticed is the DNA knot, shown in Figure 2. In the kink gas regime, one expects many reversals of alignment, and since the polymer is embedded in a three dimensional space, this can produce knot-like crossings. However, this study was limited to "phantom" bonds that could cross through each other. Nevertheless, adding a hard excluded volume potential, such as through the Heyes-Melrose algorithm,

is relatively straightforward.[7] If each bead is modelled as a hard sphere with radius comparable to the bond length, then the bead-rod chain will resemble a "pearl necklace." If the simulation timestep is sufficiently small, self-crossing of the chain can be avoided.

In an effort to reproduce the Ising force-extension curve in Cohen, we have some limited, initial data to report, as shown in Figure 4. Plotted alongside the data are the Ising force-extension relationship, the modified curve that includes thermal fluctuations, and the theoretical curve for a WLC chain. As expected, the data is well above the latter. However, the data points imperfectly fit to the middle curve. This is most likely due to a "glassy" energetic landscape, for the timescale over which chain conformation changes is very large. This also explains the low variance in extension data. Very crudely, we may estimate the longest WLC relaxation time to be on the order of the FJC Rouse relaxation time,

$$\tau = \frac{N^2 \zeta b^2}{3\pi^2 k_B T}. \tag{30}$$

For low force, chains only slowly extend over a dozen Rouse relaxation times; opening kinks is particularly difficult. This suggests kinks provide deep local potential minima. Obviously more and improved data is needed through more simulations, run for longer times. The dynamics of polymer extension in a "glassy" energetic landscape is of potential research interest.

## Conclusions

In this letter, we outlined some preliminary results from Brownian Dynamics simulations of discretised bead-rod worm-like and freely jointed chains in a high frequency AC field. These results are in line with the analytical theory derived in Cohen. Moreover, from this starting point, we may go on to investigate related problems that are analytically less tractable. An immediate step would be to include more realistic chain physics, such as long range hydrodynamic and excluded volume interactions, with the latter of particular interest in connection with observed DNA knots. We may also consider chain stretching in additional external potentials, such as would be provided by an optical trap or hard walls. Confined geometries are of special interest. Finally, we may consider more complicated chain architectures and charge distributions. However, there is still much in the framework of this study to be examined, including the theory of the kink gas, and the force-extension relationship for a polymer under traction. Further investigation is certainly warranted.


[1] C. Bustamante, Z. Bryant, and S.B. Smith, Nature **421**, 423 (2003).

[2] S.B. Smith, Y. Cui, and C. Bustamante, Science **271**, 795 (1996).

[3] H. Bruus, *Theoretical Microfluidics* (Oxford University Press, Oxford, 2008).

[4] A. Cohen, Phys. Rev. Lett. **91**, 235506 (2003).

[5] M. Somasai *et al.*, J. Non-Newtonian Fluid Mech. **108**, 227 (2002).

[6] J.F. Marko and E.D. Siggia, Macromolecules **28**, 8759 (1995).

[7] D.M. Heyes and J.R. Melrose. J. Non-Newtonian Fluid Mech. **46**, 1 (1993).